Letters

A Fast and Robust Real-Time Detection Algorithm of Decaying DC Transient and Harmonic Components in Three-Phase Systems

Liansong Xiong, *Member, IEEE*, Xiaokang Liu, Chengyong Zhao, *Senior Member, IEEE*, and Fang Zhuo, *Member, IEEE*

***Abstract*—Active power filters are conventionally utilized to compensate steady-state harmonic currents and reactive power in the utility, yet their capabilities are usually limited if the elimination of undesirable effects associated with decaying dc components during transients is the target, especially under the weak grid condition. In this letter, active cancellation of the typical first-order decaying dc-mode transients is explored. To this end, a real-time detection algorithm of decaying dc component is first developed for a generic single-phase distorted ac signal. Furthermore, fast and robust elimination of both decaying dc transient and harmonics can be performed simultaneously in three-phase grids, by adoption of moving average filters in *d–q* frame and subsequent calculations. Hardware-in-the-loop experiment results verified the effectiveness of the proposed technique.**

***Index Terms*—Active power filter (APF), decaying dc component (DDC), harmonic elimination, moving average filter (MAF), transient power quality.**

I. Introduction

THE power quality (PQ) issue has become attractive decades ago. With an increasing demand of electric power stability and reliability in sensitive facilities, e.g., the manufacturing process of electronic equipment [1], it is critical to provide continuous power supply services with high PQ in the power grid. However, both steady-state and transient PQ issues are intensively introduced to the distribution network due to the various faults, the power equipment switching and the bulk use of renewable energy generation, unbalanced/nonlinear/energy storage loads, etc., and may lead to subsequent technical and/or economic issues [2].

The increased number of impact loads has introduced transient PQ issues including voltage sag, exponentially decaying dc component (DDC), etc., especially for power supply to small rural or remote communities via weak connection to distribution network [3], or in a stand-alone power system with high penetration level of renewable energy generation [4]. Many cases, including momentary system faults, charging no-load transformers/transmission lines, grid black-start process, use of current source converters, etc., often give rise to a transient current surge and terminal voltage distortion associated with high-intensity DDC, causing possible overcurrent relay protections [5], system failures, and even black-outs.

Active power filters (APFs) have been widely used to cancel harmonics and compensate reactive power in the grid. These filters include shunt APF (SAPF), series APF, hybrid filters, and finally, unified PQ conditioner. The commonly utilized APF control methods are based on the instantaneous active and reactive theory (p–q theory) and operate well for simultaneous harmonics cancellation and reactive power compensation in balanced/unbalanced grids. However, transient PQ issues are not solved in this case, especially for DDCs elimination.

Conversely, transient PQ issues are conventionally addressed by passive devices, such as a dynamic voltage restorer, a transient voltage surge suppressor, or constant voltage transformer. It is also reported that the adoption of energy storage system with virtual impedance control [6] facilitates alleviating the impact load transient to certain extent. Though there was a steady development on the classification mechanism for power system transient disturbances [2], few attempts based on real-time active control aiming to eliminate the adverse effects of surge dynamics [7], [8] have been proposed. Besides, though some previous works (e.g., [9]–[13]) are proposed for DDC detection, it is challenging if these algorithms are utilized in real-time transient elimination, since these methods are focused on the fault type or location detection and, thus, are mainly developed for relay control and system protection. For instance, the intrinsic time-scale decomposition method [10] has certain detection

Manuscript received July 10, 2019; revised August 12, 2019; accepted September 3, 2019. Date of publication September 10, 2019; date of current version January 10, 2020. This work was supported in part by the National Natural Science Foundation of China under Grant 51707091, in part by the State Key Laboratory of Alternate Electrical Power System With Renewable Energy Sources under Grant LAPS19008, and in part by the Scientific Research Foundation for the High-Level Personnel under Grant YKJ201613. *(Corresponding author: Xiaokang Liu.)*

L. Xiong is with the School of Automation, Nanjing Institute of Technology, Nanjing 211167, China, and also with the School of Electrical Engineering, Xi'an Jiaotong University, Xi'an 710049, China (e-mail: xiongliansong@163.com).

X. Liu is with the Department of Electronics, Information, and Bioengineering, Politecnico di Milano, 20133 Milano, Italy, and also with the School of Electrical Engineering, Xi'an Jiaotong University, Xi'an 710049, China (e-mail: xiaokang.liu@polimi.it).

C. Zhao is with the State Key Laboratory of Alternate Electrical Power System With Renewable Energy Sources, North China Electric Power University, Beijing 102206, China (e-mail: chengyongzhao2@163.com).

F. Zhuo is with the School of Electrical Engineering, Xi'an Jiaotong University, Xi'an 710049, China (e-mail: zffz@mail.xjtu.edu.cn).

Color versions of one or more of the figures in this article are available online at http://ieeexplore.ieee.org.

Digital Object Identifier 10.1109/TPEL.2019.2940891

error affected by the harmonics; besides, the algorithm needs to solve nonlinear minimization problems and, therefore, has a larger computational burden. The mathematical morphology method [13] updates the output values at fixed steps (multiples of 1/2 grid cycle) and cannot track the real-time DDC continuously. The Volterra LMS/F algorithm [12] has a response time greater than one grid cycle and depends on the art of compromise, which needs parameters tuning to obtain accurate results and desired response time.

It is of paramount importance to realize real-time mode detection if the online compensation of transient PQ issue is the final goal. In this letter, a novel fast and robust detection algorithm is proposed for elimination of typical dc-mode transients in a single- or three-phase grid possibly distorted by harmonics, based on a technique similar as delayed signal cancellation [14]. For a distorted three-phase system, the harmonics during transient can be extracted simultaneously by transforming the three-phase time-domain signal into d–q quantities, and performing subsequent calculations with the adoption of moving average filters (MAFs). Consequently, this method is characterized by strong robustness against random noise and has an improved feasibility in real applications than the previous ones based on high-order time derivatives [7], [8].

The developed methodology provides twofold contributions. On one hand, the proposed DDC detection algorithm as well as the operational mode-switching scheme enables the extended functionality of conventional APFs in both static PQ control (SPQC) and transient PQ control (TPQC) scenarios. On the other hand, the outcomes of this letter can also be utilized in system phasor detection and relay protection applications, where the effect of DDC should be significantly reduced [5]; otherwise, the velocity and accuracy of faulty line selection can be notably degraded.

II. DDC Transient and Harmonic Detection

In this section, a novel real-time detection algorithm of the DDC is first developed for a single-phase harmonic distorted system, yet can be utilized for a three-phase system as well by performing simultaneous calculations on each phase. Subsequently, the fast and robust detection algorithm of both DDC transient and harmonics is developed for a three-phase system.

A. Detection of DC Component in Single-Phase System

For ease of notation, a DDC-mode transient component is imposed on the grid current with odd-order harmonic distortion at the time instant $t = 0$. Consequently, current values sampled at time t, $t - T/2$, and $t - T$ (for $t \geq T$) during the transient are expressed as

$$i_{\text{tr}}(t) = I_0 \sin(\omega t + \varphi_0) + I_{\text{dc}} e^{-\sigma t} + \sum_{n=3,5,7,\ldots} I_n \sin(n\omega t + \varphi_n) \tag{1}$$

$$i_{\text{tr}}\left(t - \tfrac{T}{2}\right) = -I_0 \sin(\omega t + \varphi_0) + I_{\text{dc}} e^{-\sigma t} e^{\frac{\sigma T}{2}} - \sum I_n \sin(n\omega t + \varphi_n) \tag{2}$$

$$i_{\text{tr}}(t - T) = I_0 \sin(\omega t + \varphi_0) + I_{\text{dc}} e^{-\sigma t} e^{\sigma T} + \sum_{n=3,5,7,\ldots} I_n \sin(n\omega t + \varphi_n) \tag{3}$$

where T is the utility period, I_0, ω, and φ_0 are the amplitude, radian frequency, and initial phase of the fundamental ac component, respectively. I_n and φ_n are the amplitude and initial phase of the nth order harmonic component, respectively. I_{dc} and σ are the amplitude and damping constant of the transient dc component, respectively. Accordingly, we have

$$i_{\text{tr}}(t) + i_{\text{tr}}\left(t - \frac{T}{2}\right) = I_{\text{dc}} e^{-\sigma t}\left(1 + e^{\frac{\sigma T}{2}}\right) \tag{4}$$

$$i_{\text{tr}}(t) - i_{\text{tr}}(t - T) = I_{\text{dc}} e^{-\sigma t}\left(1 - e^{\sigma T}\right). \tag{5}$$

By combining (4) and (5), the DDC transient current can be extracted as

$$i_{\text{DDC}}(t) = I_{\text{dc}} e^{-\sigma t} = \frac{\left[i_{\text{tr}}(t) + i_{\text{tr}}\left(t - \frac{T}{2}\right)\right]^2}{i_{\text{tr}}(t) + i_{\text{tr}}(t - T) + 2 i_{\text{tr}}\left(t - \frac{T}{2}\right)}. \tag{6}$$

B. Simultaneous Detection of DC and Harmonic Components in Three-Phase System

The generic three-phase current signals, distorted by odd-order harmonics and unbalanced decaying dc transient components starting at $t = 0$, are defined as

$$i^a_{\text{tr}}(t) = I_0 \sin(\omega t + \varphi_0) + I^a_{\text{dc}} e^{-\sigma t} + \sum_{n=3,5,7,\ldots} I_n \sin(n\omega t + \varphi_n) \tag{7}$$

$$i^b_{\text{tr}}(t) = I_0 \sin(\omega t + \varphi_0 - 2\pi/3) + I^b_{\text{dc}} e^{-\sigma t} + \sum_{n=3,5,7,\ldots} I_n \sin(n\omega t + \varphi_n - 2\pi/3) \tag{8}$$

$$i^c_{\text{tr}}(t) = I_0 \sin(\omega t + \varphi_0 + 2\pi/3) + I^c_{\text{dc}} e^{-\sigma t} + \sum_{n=3,5,7,\ldots} I_n \sin(n\omega t + \varphi_n + 2\pi/3). \tag{9}$$

The three-phase transient currents in the a–b–c frame can be transformed to rotational d–q frame quantities via Park transformation as

$$\begin{bmatrix} i^d_{\text{tr}}(t) \\ i^q_{\text{tr}}(t) \end{bmatrix} = \mathbf{T}_{abc/dq} \begin{bmatrix} i^a_{\text{tr}}(t) \\ i^b_{\text{tr}}(t) \\ i^c_{\text{tr}}(t) \end{bmatrix} \tag{10}$$

where

$$\mathbf{T}_{abc/dq} = \frac{2}{3} \begin{bmatrix} \sin\omega t & \sin\left(\omega t - \frac{2\pi}{3}\right) & \sin\left(\omega t + \frac{2\pi}{3}\right) \\ \cos\omega t & \cos\left(\omega t - \frac{2\pi}{3}\right) & \cos\left(\omega t + \frac{2\pi}{3}\right) \end{bmatrix}. \tag{11}$$

The resultant d–q frame quantities are

$$i^d_{\text{tr}}(t) = I_0 \cos\varphi_0 + I_{\text{DC}} \sin(\omega t + \gamma_d) e^{-\sigma t} + \sum_{n=3,5,7,\ldots} I_n \cos[(n-1)\omega t + \varphi_n] \tag{12}$$

$$i^q_{\text{tr}}(t) = I_0 \sin\varphi_0 + I_{\text{DC}} \sin(\omega t + \gamma_q) e^{-\sigma t} + \sum I_n \sin[(n-1)\omega t + \varphi_n] \tag{13}$$

where

$$\begin{cases} I_{\rm DC} = \dfrac{1}{3}\sqrt{\left(2I^a_{\rm dc} - I^b_{\rm dc} - I^c_{\rm dc}\right)^2 - 3\left(I^b_{\rm dc} - I^c_{\rm dc}\right)^2} \\ \tan\gamma_d = -\dfrac{\sqrt{3}\left(I^b_{\rm dc} - I^c_{\rm dc}\right)}{2I^a_{\rm dc} - I^b_{\rm dc} - I^c_{\rm dc}} \\ \tan\gamma_q = \dfrac{2I^a_{\rm dc} - I^b_{\rm dc} - I^c_{\rm dc}}{\sqrt{3}\left(I^b_{\rm dc} - I^c_{\rm dc}\right)}. \end{cases} \tag{14}$$

It is seen that the transient d, q current quantities are comprised of three portions: 1) constant components dependent on the base-frequency amplitude I_0 and phase shift φ_0; 2) even-order harmonics, originated from the odd-order harmonics in the stationary domain (with deduction of orders by 1); and 3) decaying sinusoidal components arised from the three-phase dc components.

By time integration of (12) for one power cycle and half power cycle, respectively, we have (15) and (16) shown at the bottom of this page. Consequently, the constant component in (12) can be obtained as

$$I_0\cos\varphi_0 = 2\frac{\int_{t-T}^{t} i^d_{\rm tr}(t)dt + \left(e^{\frac{T\sigma}{2}} - 1\right)\int_{t-\frac{T}{2}}^{t} i^d_{\rm tr}(t)dt}{T\left(1 + e^{\frac{T\sigma}{2}}\right)}. \tag{17}$$

Similarly, the first component in (13) yields

$$I_0\sin\varphi_0 = 2\frac{\int_{t-T}^{t} i^q_{\rm tr}(t)dt + \left(e^{\frac{T\sigma}{2}} - 1\right)\int_{t-\frac{T}{2}}^{t} i^q_{\rm tr}(t)dt}{T\left(1 + e^{\frac{T\sigma}{2}}\right)}. \tag{18}$$

The summation of DDC and harmonic components are then calculated as the residual parts in (12) and (13) and, thus, can be served as the compensation current reference for active transient cancellation.

III. Applications to Active Transient Cancellation

For the implementation of discrete-time active dc transient elimination, a constant sampling time T_s is considered. The DDC detection algorithm in a single-phase system (6) can be reformulated as a discrete sequence, yielding

$$\hat{i}_{\rm DDC}(k) = \frac{\left[\hat{i}_{\rm tr}(k) + \hat{i}_{\rm tr}(k-N)\right]^2}{\hat{i}_{\rm tr}(k) + \hat{i}_{\rm tr}(k-2N) + 2\hat{i}_{\rm tr}(k-N)} \tag{19}$$

where k is the discrete-time step, symbol $\hat{}$ represents the corresponding discrete sequence, and $N = \text{round}(0.5T/T_s)$ is the number of sample points for half power cycle.

By adopting the notations of an MAF (see [14, eq. (11)]), the counterparts of three-phase base-frequency components in d–q frame, (17) and (18), can be rewritten as

$$I_0\cos\varphi_0 = \frac{2\left[\hat{i}_{\rm tr}(k)+\hat{i}_{\rm tr}(k-N)\right]\bar{\hat{i}}^d_{\rm tr,1}(k) - \left[\hat{i}_{\rm tr}(k)-\hat{i}_{\rm tr}(k-2N)\right]\bar{\hat{i}}^d_{\rm tr,2}(k)}{\hat{i}_{\rm tr}(k) + 2\hat{i}_{\rm tr}(k-N) + \hat{i}_{\rm tr}(k-2N)} \tag{20}$$

$$I_0\sin\varphi_0 = \frac{2\left[\hat{i}_{\rm tr}(k)+\hat{i}_{\rm tr}(k-N)\right]\bar{\hat{i}}^q_{\rm tr,1}(k) - \left[\hat{i}_{\rm tr}(k)-\hat{i}_{\rm tr}(k-2N)\right]\bar{\hat{i}}^q_{\rm tr,2}(k)}{\hat{i}_{\rm tr}(k) + 2\hat{i}_{\rm tr}(k-N) + \hat{i}_{\rm tr}(k-2N)} \tag{21}$$

respectively, where $\bar{\hat{i}}^{d,q}_{{\rm tr},n}(k)$ denotes the d- and q-axis MAF quantities for eliminating the nth harmonic (i.e., $n = 1$ and 2 correspond to the MAFs with periods of 1 and 0.5 power cycle, respectively).

In addition, a steady-state signal SS (SS $= 1$ corresponds to the steady-state scenario) can be obtained using the criterion

$$\text{SS} = \begin{cases} 1, \text{ if } \hat{i}_{\rm tr}(k) = \hat{i}_{\rm tr}(k-2N) \text{ and } \hat{i}_{\rm tr}(k) = -\hat{i}_{\rm tr}(k-N) \\ 0, \text{ otherwise.} \end{cases} \tag{22}$$

Note that (19)–(21) are valid in the presence of a DDC-mode transient. In the scenario when the steady-state condition is satisfied, the extraction algorithm should be disabled to avoid numerical instabilities which might otherwise introduce inrush current references, and conventional active cancellation algorithms should be adopted. Several measures can be taken to improve the transient detection reliability, e.g., considering the noise margin introduced by the current sampling system, and selecting the phase signal with largest DDC in (20) and (21) to provide the largest signal-to-noise ratio.

A complete diagram for the APF operating with simultaneous SPQC and TPQC abilities (denoted as hybrid-mode control hereinafter) is shown in Fig. 1. Though the moving average d- and q-axis currents are used in the SPQC mode here, it is noted that other SPQC algorithms (e.g., implementations based on instantaneous power theory) can be adopted as well in the control module of the active-filtering equipment. The SPQC and TPQC control modes are dynamically altered according to the real-time load current signals. An illustration of two hybrid working modes is shown in Fig. 2.

The overall dynamic response time of the proposed method is theoretically one grid period due to the presence of MAF1 blocks in the control module (see Fig. 1). During the initial grid cycle of transient process, the APF can either be operated in the SPQC mode for reduced dc-side capacitor sizing, or TPQC

$$\int_{t-T}^{t} i^d_{\rm tr}(t)dt = I_0 T\cos\varphi_0 + \frac{I_{\rm DC}e^{-\sigma t}\left(e^{\sigma T} - 1\right)\left[\omega\cos\left(\omega t + \gamma_d\right) + \sigma\sin\left(\omega t + \gamma_d\right)\right]}{\sigma^2 + \omega^2} \tag{15}$$

$$\int_{t-\frac{T}{2}}^{t} i^d_{\rm tr}(t)dt = I_0\frac{T}{2}\cos\varphi_0 - \frac{I_{\rm DC}e^{-\sigma t}\left(e^{\sigma\frac{T}{2}} + 1\right)\left[\omega\cos\left(\omega t + \gamma_d\right) + \sigma\sin\left(\omega t + \gamma_d\right)\right]}{\sigma^2 + \omega^2} \tag{16}$$

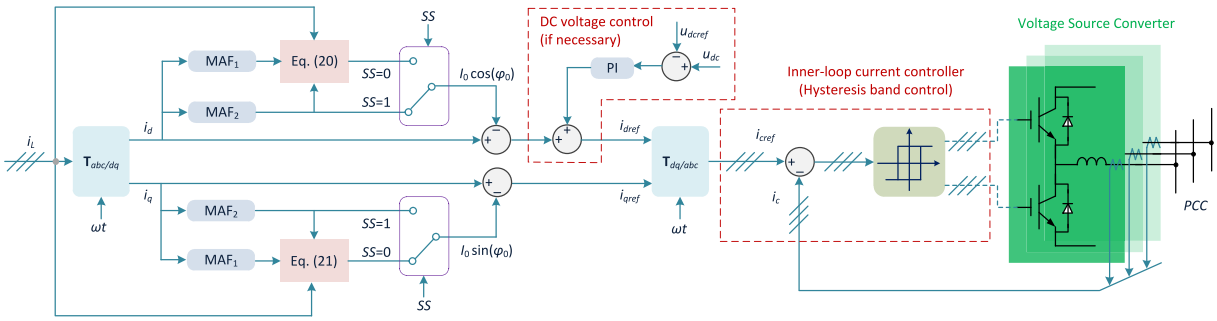

Fig. 1. Block diagram for simultaneous active SPQC and TPQC. A incremental MAF block implementation can be found in [15, Fig. 3].

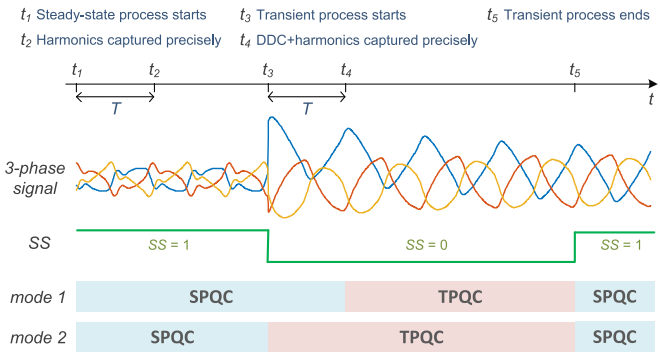

Fig. 2. Illustration of proposed APF hybrid working modes.

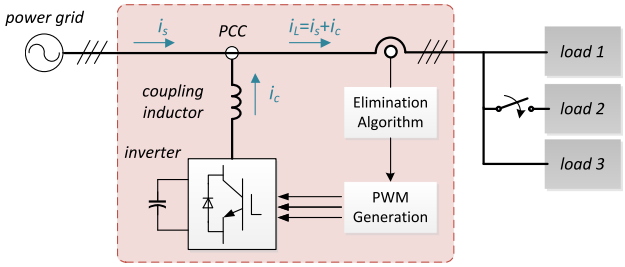

Fig. 3. Circuit topology used for experiment.

mode for improved transient elimination performance (which might be more appealing if the stable system operation is a priority).

IV. Experimental Verification

To illustrate the effectiveness of the proposed methodology under different operational conditions, in this section, a three-phase SAPF, conventionally utilized to inject compensating harmonic currents into the power system to mitigate harmonic currents generated by nonlinear loads, is used also for transient current compensation (see Fig. 3 for the system topology). The SAPF is connected at the point of common coupling (PCC) of three-phase lines, with the power grid and loads at different terminals. Without loss of generality, three loads are used in the experiment: load 1 is a controlled harmonic current source modeling the nonlinear behavior of

TABLE I
System Parameters

Parameter	Value	Parameter	Value
Three-phase voltage (ph-ph)	380 Vrms	Base frequency	50 Hz
Coupling inductor	20 mH	Load 2	2 Ω + 0.1 H
Nominal DC voltage	1 000 V	Load 3	500 Ω + 2 H
Nominal DC capacitance	3 300 μF		

loads, loads 2 and 3 are both series R–L loads representing the generic inductive load behavior of power systems, and a three-phase breaker (initially open and suddenly closes) is used to model the switching of loads. System parameters are listed in Table I.

Different APF control schemes, i.e., SPQC-mode and hybrid-mode control (as shown in Fig. 2) strategies are utilized and compared for the same transient. Apart from the proposed technique, a PI controller ($K_P = 0.08$; $K_I = 0.2$) is utilized for dc-side voltage regulation, and a hysteresis band controller is adopted for inner current control. The experiment results for load and grid currents are shown in Fig. 4, and the dc-side voltage under different operation modes are illustrated in Fig. 5. In addition to the three-phase signals, a breaker status signal (see green curves in Figs. 4 and 5, where low and high voltage levels indicate breaker open and close status, respectively) is utilized for better visualization of the transition process (note that the breaker status signal is not equivalent to SS, which is generated by the steady-state criterion (22) according to the real-time current sampling). It is evident that the conventional SPQC-mode is insufficient in eliminating DDC-mode transients, where unbalanced three-phase currents are supplied from the power source, inducing negative impacts to the grid. The proposed hybrid-mode compensation scheme, on the contrary, is characterized by the fast dynamic response and extended functionality to eliminate both transient and harmonic components simultaneously. If the APF is operated with the delayed TPQC during dynamic process, the grid will observe a maximum impact current in the first transient cycle [see Fig. 4(c)]; on the contrary, the adoption of immediate TPQC during transient provides an unchanged grid current amplitude in the first half-cycle (due to the constant calculation results of (20) and (21) in this time slot), then rapid, smooth grid current transition where the spike current disturbance is avoided [see Fig. 4(d)].

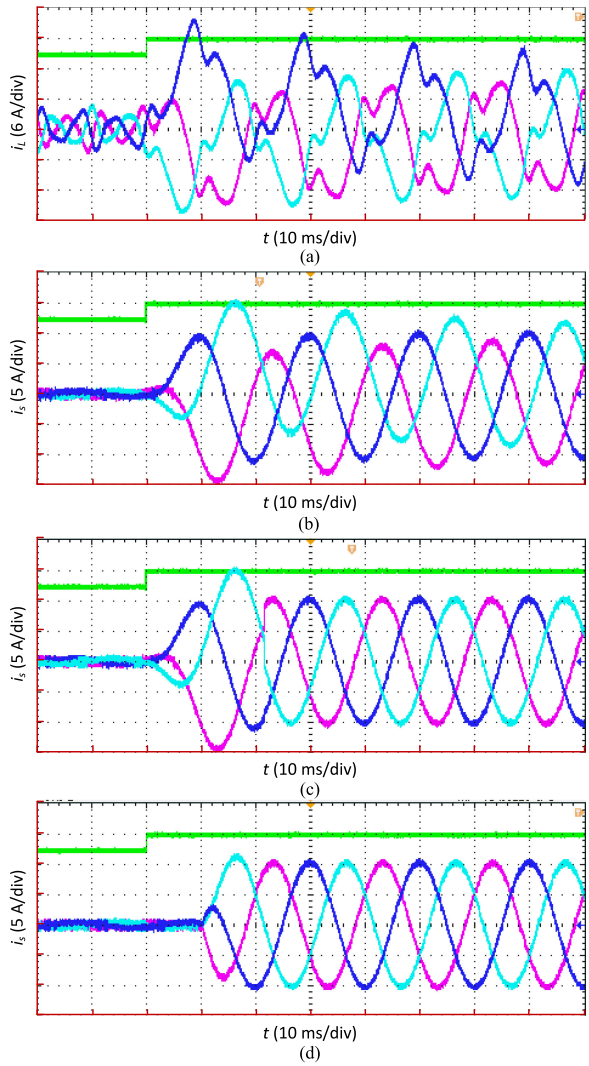

Fig. 4. Experiment results for (a) three-phase load current; current from power grid when SAPF operates in (b) SPQC-only mode, (c) hybrid mode 1, and (d) hybrid mode 2.

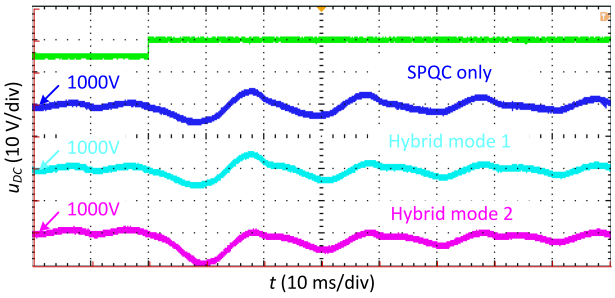

Fig. 5. Experimental results for dc-side voltages with different control strategies.

V. Conclusion

In this letter, a novel fast and robust detection algorithm was proposed for elimination of typical dc-mode surge transients in ac grids possibly distorted by harmonics. For a harmonic-distorted three-phase system, the harmonic components, as well as the transient dc components could be simultaneously alleviated, as confirmed by experiment results.

The developed algorithm was among the pioneering works to efficiently and actively mitigating transient PQ issues, and was advantageous to mitigate transient PQ issues in practical applications owing to its strong robustness against random system noise, overcoming the limitations of the previous technique [8]. The proposed hybrid-mode control scheme could be readily embedded in the control module of conventional APFs and similar voltage source converter (VSC) devices (e.g., inverters in photovoltaic/wind power generation systems, converters in VSC-type high-voltage dc systems) to deal with the DDC-related technical issues, extending the device functionality to both steady-state and transient operations without extra hardware costs.

References

[1] K. Olikara, "Power quality issues, impacts, and mitigation for industrial customers," pp. 1–7, Sep. 2015. [Online]. Available: https://literature.rockwellautomation.com/idc/groups/literature/documents/wp/power-wp002_-en-p.pdf

[2] R. Ahila, V. Sadasivam, and K. Manimala, "An integrated PSO for parameter determination and feature selection of ELM and its application in classification of power system disturbances," *Appl. Soft Comput.*, vol. 32, pp. 23–37, 2015.

[3] Y. Tan, L. Meegahapola, and K. M. Muttaqi, "A review of technical challenges in planning and operation of remote area power supply systems," *Renew. Sustain. Energy Rev.*, vol. 38, pp. 876–889, 2014.

[4] L. Xiong *et al.*, "Static synchronous generator model: A new perspective to investigate dynamic characteristics and stability issues of grid-tied PWM inverter," *IEEE Trans. Power Electron.*, vol. 31, no. 9, pp. 6264–6280, Sep. 2016.

[5] N. T. Stringer, "The effect of DC offset on current-operated relays," *IEEE Trans. Ind. Appl.*, vol. 34, no. 1, pp. 30–34, Jan./Feb. 1998.

[6] C. Sun, G. Joos, and F. Bouffard, "Adaptive coordination for power and SoC limiting control of energy storage in islanded AC microgrid with impact load," *IEEE Trans. Power Del.*, to be published, doi: 10.1109/TPWRD.2019.2916034.

[7] M. Zhu *et al.*, "A novel method for modeling of dc micro-grid based on characteristic parameter," in *Proc. IEEE Appl. Power Electron. Conf. Expo.*, 2014, pp. 3465–3468.

[8] L. Xiong, C. Li, F. Zhuo, M. Zhu, B. Liu, and H. Zhang, "A novel real-time and on-line computation algorithm for characteristic parameters of micro-grids," in *Proc. IEEE Appl. Power Electron. Conf. Expo.*, 2014, pp. 427–431.

[9] Z. Jiang, S. Miao, and P. Liu, "A modified empirical mode decomposition filtering-based adaptive phasor estimation algorithm for removal of exponentially decaying DC offset," *IEEE Trans. Power Del.*, vol. 29, no. 3, pp. 1326–1334, Jun. 2014.

[10] M. Pazoki, "A new DC-offset removal method for distance-relaying application using intrinsic time-scale decomposition," *IEEE Trans. Power Del.*, vol. 33, no. 2, pp. 971–980, Apr. 2018.

[11] B. Jafarpisheh, S. M. Madani, and S. Jafarpisheh, "Improved DFT-based phasor estimation algorithm using down-sampling," *IEEE Trans. Power Del.*, vol. 33, no. 6, pp. 3242–3245, Dec. 2018.

[12] U. Subudhi, H. K. Sahoo, and S. K. Mishra, "Harmonics and decaying DC estimation using volterra LMS/F algorithm," *IEEE Trans. Ind. Appl.*, vol. 54, no. 2, pp. 1108–1118, Mar./Apr. 2018.

[13] K. Zhu and P. W. T. Pong, "Fault classification of power distribution cables by detecting decaying DC components with magnetic sensing," *IEEE Trans. Instrum. Meas.*, to be published, doi: 10.1109/TIM.2019.2922514.

[14] L. Xiong, F. Zhuo, F. Wang, X. Liu, M. Zhu, and H. Yi, "A quantitative evaluation and comparison of harmonic elimination algorithms based on moving average filter and delayed signal cancellation in phase synchronization applications," *J. Power Electron.*, vol. 16, no. 2, pp. 717–730, 2016.

[15] S. Golestan, M. Ramezani, J. M. Guerrero, F. D. Freijedo, and M. Monfared, "Moving average filter based phase-locked loops: Performance analysis and design guidelines," *IEEE Trans. Power Electron.*, vol. 29, no. 6, pp. 2750–2763, Jun. 2014.